

# Investigation of Dynamic Fracture Behavior in Functionally Graded Materials Using the Interaction Integral Method

Seong Hyeok Song<sup>a</sup> and Glaucio H. Paulino<sup>b</sup>

<sup>a</sup> *Structure Design, Division of Engineering Services, Department of Transportation, 1801 30th Street  
M.S. 9-3/3G, Sacramento, CA 95833, U.S.A.*

<sup>b</sup> *Department of Civil and Environmental Engineering, University of Illinois at Urbana-Champaign,  
205 North Mathews Avenue, Urbana, IL 61801, U.S.A.*

**Abstract.** Dynamic stress intensity factor (DSIF) is an important fracture parameter in understanding and predicting dynamic fracture behavior of a cracked body. To evaluate DSIFs for functionally graded materials (FGMs), the interaction integral originally proposed to evaluate SIFs for a static homogeneous medium is extended to incorporate dynamic effects and material nonhomogeneity, and is implemented in conjunction with the finite element method (FEM). To verify numerical implementations and to explore various dynamic fracture behaviors, both homogeneous and nonhomogeneous cracked bodies under dynamic loading are employed.

**Keywords:** dynamic stress intensity factors (DSIFs), functionally graded materials, interaction integral, fracture.

## INTRODUCTION

Static and dynamic fracture behaviors of homogeneous and nonhomogeneous cracked bodies can be understandable and predictable once stress intensity factors (SIFs) are known. Thus, an accurate evaluation of SIFs is crucial in fracture mechanics for both static and dynamic cases as they are closely associated with crack initiation and propagation.

For homogeneous materials, Chen [1] examined a centrally cracked rectangular finite strip subjected to step loading using a Lagrangian finite difference method (FDM). DSIFs were obtained from the relation between DSIFs and stress fields in the vicinity of a crack tip. Several researchers have investigated dynamic fracture behavior using various theoretical and numerical techniques [2,3,4,5,6].

For nonhomogeneous materials, Rousseau and Tippur obtained DSIFs for functionally graded materials (FGMs) both numerically and experimentally [7]. The DSIFs prior to crack initiation were determined utilizing asymptotic fields of Williams' solution [8], which is equivalent to the stationary fields. After initiation, the crack tip fields for steadily growing cracks in FGMs obtained by Parameswaran and Shukla [9] were used to obtain DSIFs. Material gradients were employed in the commercial software ABAQUS [10] by applying temperature, which is a function of material properties, and by letting the coefficient of thermal expansion be zero. As the distance is close to the crack tip, the DSIFs were underestimated because no singular

CP973, *Multiscale and Functionally Graded Materials 2006*

edited by G. H. Paulino, M.-J. Pindera, R. H. Dodds, Jr., F. A. Rochinha, E. V. Dave, and L. Chen

© 2008 American Institute of Physics 978-0-7354-0492-2/08/\$23.00

elements were used. Therefore, regression technique was employed to obtain DSIFs at the crack tip based on the DCT. Wu et al. [11] extended the J-integral to incorporate material gradients and dynamic effects.

Although a few researchers [7,11] evaluated fracture quantities such as SIFs or J for nonhomogeneous cracked bodies under dynamic loading, only mode I SIF, i.e.  $K_I$ , is evaluated in conjunction with either the J-integral or the DCT. So, the motivation of this study follows: 1) The interaction integral (M-integral), which is known to be superior to the DCT and J-integral, is extended to incorporate material nonhomogeneity and dynamic effects for evaluation of DSIFs; and 2) A mixed-mode nonhomogeneous medium under dynamic loadings is adopted to compute dynamic  $K_I$  and  $K_{II}$ .

## INTERACTION INTEGRAL

In this section, the interaction integral is formulated by superimposing the actual and auxiliary fields on the path independent J-integral. A M-integral is derived based on a non-equilibrium formulation.

The J-integral is

$$J = \int_A \left( \sigma_{ij} u_{i,1} - \frac{1}{2} \sigma_{ik} \varepsilon_{ik} \delta_{1j} \right) q_{,j} dA + \int_A \left( \sigma_{ij,j} u_{i,1} + \sigma_{ij} u_{i,1j} - \frac{1}{2} \sigma_{ij,1} \varepsilon_{ij} - \frac{1}{2} \sigma_{ij} \varepsilon_{ij,1} \right) q dA. \quad (1)$$

in which  $\sigma$  and  $\varepsilon$  denote stress and strain, respectively;  $\delta$  stands for Kronecker Delta;  $\mathbf{u}$  represents displacement; and  $q$  is a function varying from 0 to 1. Superimposing the actual and auxiliary fields on Eq. (1), one obtains

$$J^s = \int_A \left\{ (\sigma_{ij}^{aux} + \sigma_{ij}) (u_{i,1}^{aux} + u_{i,1}) - \frac{1}{2} (\sigma_{ik}^{aux} + \sigma_{ik}) (\varepsilon_{ik}^{aux} + \varepsilon_{ik}) \delta_{1j} \right\} q_{,j} dA + \int_A \left\{ (\sigma_{ij,j}^{aux} + \sigma_{ij,j}) (u_{i,1}^{aux} + u_{i,1}) + (\sigma_{ij}^{aux} + \sigma_{ij}) (u_{i,1j}^{aux} + u_{i,1j}) \right\} q dA - \frac{1}{2} \int_A \left\{ (\sigma_{ij,1}^{aux} + \sigma_{ij,1}) (\varepsilon_{ij}^{aux} + \varepsilon_{ij}) + (\sigma_{ij}^{aux} + \sigma_{ij}) (\varepsilon_{ij,1}^{aux} + \varepsilon_{ij,1}) \right\} q dA, \quad (2)$$

which is decomposed into

$$J^s = J + J^{aux} + M, \quad (3)$$

where  $J$  is provided in Eq. (1) and  $J^{aux}$  is expressed as follows

$$J^{aux} = \int_A \left( \sigma_{ij}^{aux} u_{i,1} - \frac{1}{2} \sigma_{ik}^{aux} \varepsilon_{ik}^{aux} \delta_{1j} \right) q_{,j} dA + \int_A \left( \sigma_{ij,j}^{aux} u_{i,1}^{aux} + \sigma_{ij}^{aux} u_{i,1j}^{aux} - \frac{1}{2} \sigma_{ij,1}^{aux} \varepsilon_{ij}^{aux} - \frac{1}{2} \sigma_{ij}^{aux} \varepsilon_{ij,1}^{aux} \right) q dA. \quad (4)$$

The resulting M integral is given by

$$\begin{aligned}
M = & \int_A \left\{ \sigma_{ij}^{aux} u_{i,1} + \sigma_{ij} u_{i,1}^{aux} - \frac{1}{2} (\sigma_{ik}^{aux} \varepsilon_{ik} + \sigma_{ik} \varepsilon_{ik}^{aux}) \delta_{1j} \right\} q_{,j} dA \\
& + \int_A \left\{ (\sigma_{ij}^{aux} u_{i,1} + \sigma_{ij,j} u_{i,1}^{aux}) + (\sigma_{ij}^{aux} u_{i,1,j} + \sigma_{ij} u_{i,1,j}^{aux}) \right\} q dA \\
& - \frac{1}{2} \int_A \left\{ (\sigma_{ij,1}^{aux} \varepsilon_{ij} + \sigma_{ij,1} \varepsilon_{ij}^{aux}) + (\sigma_{ij}^{aux} \varepsilon_{ij,1} + \sigma_{ij} \varepsilon_{ij,1}^{aux}) \right\} q dA
\end{aligned} \tag{5}$$

Among three formulations which are based on non-equilibrium, incompatibility and constant constitutive tensor, the non-equilibrium formulation is employed in this study. Since the actual fields adopt the quantities obtained from numerical simulations, the equilibrium and compatibility condition are satisfied, i.e.,

$$\sigma_{ij,j} = \rho \ddot{u}_i \tag{6}$$

$$\varepsilon_{ij} = \frac{1}{2} (u_{i,j} + u_{j,i}), \quad \sigma_{ij} u_{i,1,j} = \sigma_{ij} \varepsilon_{ij,1}, \tag{7}$$

in which  $\rho$  is mass density and  $\ddot{u}$  refers to acceleration.

For the auxiliary fields, the equilibrium condition is not satisfied, i.e.,

$$\sigma_{ij,j}^{aux} \neq 0, \tag{8}$$

while the relation between strain and displacement is compatible:

$$\varepsilon_{ij}^{aux} = \frac{1}{2} (u_{i,j}^{aux} + u_{j,i}^{aux}), \quad \sigma_{ij} u_{i,1,j}^{aux} = \sigma_{ij} \varepsilon_{ij,1}^{aux} \tag{9}$$

Note that the auxiliary fields are chosen as asymptotic fields for static homogeneous materials. For the superimposed actual and auxiliary fields, the following equalities are obtained:

$$\sigma_{ij} \varepsilon_{ij}^{aux} = C_{ijkl}(\mathbf{x}) \varepsilon_{kl} \varepsilon_{ij}^{aux} = \sigma_{kl}^{aux} \varepsilon_{kl} = \sigma_{ij}^{aux} \varepsilon_{ij}, \tag{10}$$

$$C_{ijkl,1}(\mathbf{x}) \varepsilon_{kl}^{aux} \varepsilon_{ij} = C_{ijkl,1}(\mathbf{x}) \varepsilon_{ij}^{aux} \varepsilon_{kl} \tag{11}$$

$$C_{ijkl}(\mathbf{x}) = \varepsilon_{kl,1} \varepsilon_{ij}^{aux} = \sigma_{ij}^{aux} \varepsilon_{ij,1} \tag{12}$$

$$C_{ijkl}(\mathbf{x}) \varepsilon_{kl,1} \varepsilon_{ij} = \sigma_{ij} \varepsilon_{ij,1} \tag{13}$$

$$\sigma_{ij,1}^{aux} \varepsilon_{ij} = (C_{ijkl}(\mathbf{x}) \varepsilon_{kl}^{aux})_{,1} \varepsilon_{ij} = (C_{ijkl,1}(\mathbf{x}) \varepsilon_{kl}^{aux} + C_{ijkl}(\mathbf{x}) \varepsilon_{kl,1}^{aux}) \varepsilon_{ij} \tag{14}$$

$$\sigma_{ij,1} \varepsilon_{ij}^{aux} = (C_{ijkl}(\mathbf{x}) \varepsilon_{kl})_{,1} \varepsilon_{ij}^{aux} = (C_{ijkl,1}(\mathbf{x}) \varepsilon_{kl} + C_{ijkl}(\mathbf{x}) \varepsilon_{kl,1}) \varepsilon_{ij}^{aux}, \tag{15}$$

where  $\mathbf{C}$  denotes the elasticity tensor.

Using the equalities, one obtains the M-integral as follows

$$\begin{aligned}
M = & \int_A \left\{ (\sigma_{ij}^{aux} u_{i,1} + \sigma_{ij} u_{i,1}^{aux}) - \sigma_{ik}^{aux} \varepsilon_{ik} \delta_{1j} \right\} q_{,j} dA \\
& + \int_A \left\{ (\sigma_{ij,j}^{aux} u_{i,1} + \rho \ddot{u}_i u_{i,1}^{aux} - C_{ijkl,1} \varepsilon_{kl}^{aux} \varepsilon_{ij}) \right\} q dA
\end{aligned} \tag{16}$$

where  $\sigma_{ij,j}^{aux} u_{i,1}$ ,  $\rho \ddot{u}_i u_{i,1}^{aux}$  and  $C_{ijkl,1} \varepsilon_{kl}^{aux} \varepsilon_{ij}$  appear due to non-equilibrium condition of the auxiliary fields, dynamic effect of the actual fields, and material nonhomogeneity of the actual fields, respectively. If dynamic effects are ignored, this equation reduces to the interaction integral for the static nonhomogeneous material case derived by Kim

and Paulino [12]. Other formulations and detailed numerical implement procedures can be found in the references [13, 14].

## COMPUTATIONAL RESULTS

Fedelinski et al. [15] used the dual BEM and  $\hat{J}$  integral to determine DSIFs in a rectangular plate with cracks emanating from a circular hole. A decomposition procedure was employed for mode mixity. Various angles which range from  $0^\circ$  to  $60^\circ$  were adopted to investigate fracture behavior in terms of the variation of DSIFs. In this study, a crack angle  $30^\circ$  is chosen to verify DSIFs for homogeneous materials and to investigate the influence of material gradation on DSIFs for FGMs. Figure 1 (a) illustrates a rectangular finite plate with a width  $2W=30$  mm and a height  $2H=60$  mm containing a hole of radius  $r=3.75$  mm. Two cracks extend from the hole, and the length between the two crack tips is 15mm. The cracks are inclined at  $30^\circ$  clockwise from horizontal. Figures 1 (b), (c) and (d) show the mesh configurations for the whole geometry, and mesh details near the hole and the crack tip. A crack tip template of 12 sectors and 4 rings of elements provides sufficient mesh refinement around the crack tip regions, which is crucial for reliable numerical results. Step loading is applied to both the top and bottom edges. No other boundary conditions are prescribed. In this mesh, 1350 Q8 and 204 T6 plane strain elements are used with  $3 \times 3$  Gauss quadrature. The average acceleration method is adopted with a time step of  $\Delta t=0.1\mu s$ , and consistent mass matrix is employed.

### Verification

A comparison between the present numerical results and the reference solution for the homogeneous case is performed to verify the numerical techniques implemented in this study. The following material properties are used:  $E=199.992$  GPa,  $\rho=5000$  Kg/m<sup>3</sup> and  $\nu=0.3$ . Figure 2 shows the comparison between the present numerical results and the reference solution [15] at the right crack tip. The reference results plotted here are obtained from graphical data using special-purpose software. The abscissa indicates time up to 20  $\mu s$ . The DSIFs are normalized by  $K_s = \sigma_0 \sqrt{\pi a}$  in which  $\sigma_0$  is the magnitude of the applied stress. The present numerical results agree well with the reference solution. Greater but acceptable difference is found between  $K_I(t)$  values than between  $K_{II}(t)$  values. The difference may be attributed to different numerical schemes, different domain discretizations, and different conservation integrals.

### Nonhomogeneous Plate

Real nonhomogeneous material properties prepared by Rousseau and Tippur [7] are adopted to investigate fracture behavior. Rousseau and Tippur [7] prepared three point bending specimens made of epoxy and solid soda-lime glass spheres. The material properties of the current specimen follow the values provided in Rousseau and Tippur [7] and assume linear variation of material properties in the  $x$  direction, described by

$$E(x) = (244x + 7471)(MPa) \quad (17)$$

$$\rho(x) = (28.8x + 1380)(Kg / m^3) \quad (18)$$

A constant Poisson's ratio of 0.3 is used.

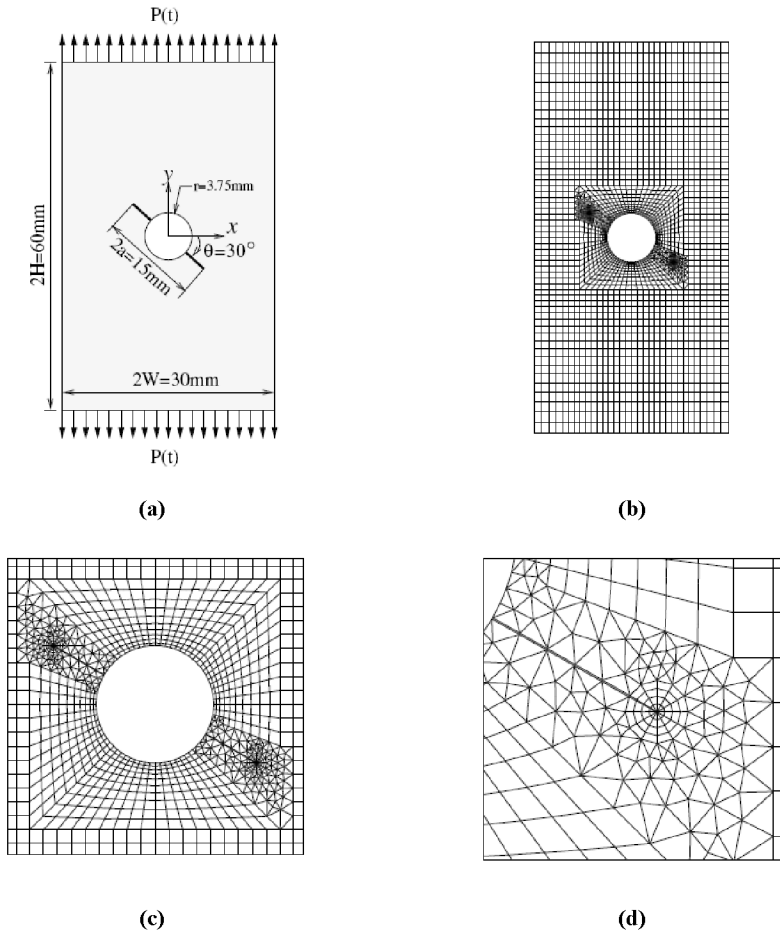


**FIGURE 1.** Rectangular plate with cracks emanating from a circular hole: (a) geometry and boundary conditions; (b) mesh configuration for the whole geometry; (c) mesh details for both crack tip regions; and (d) mesh details for the right crack tip (12 sectors and 4 rings)

Normalized mixed-mode DSIFs versus time curves at both the right and left crack tip locations are plotted in Figure 3. The ordinate indicates DSIFs normalized by  $K_S$  and the abscissa is time up to  $40 \mu s$ . Since initiation time of DSIFs depends on the dilatational wave speed, first the DSIFs at the right crack tip initiate, and then, the DSIFs at the left crack tip initiate as shown in Figure 3. At any given time of the transient response, the magnitude of  $K_I(t)$  at the right crack tip is higher than that at the

left crack tip for the nonhomogeneous case. This is due to the fact that the values of material properties at the right crack tip are higher than those at the left crack tip.

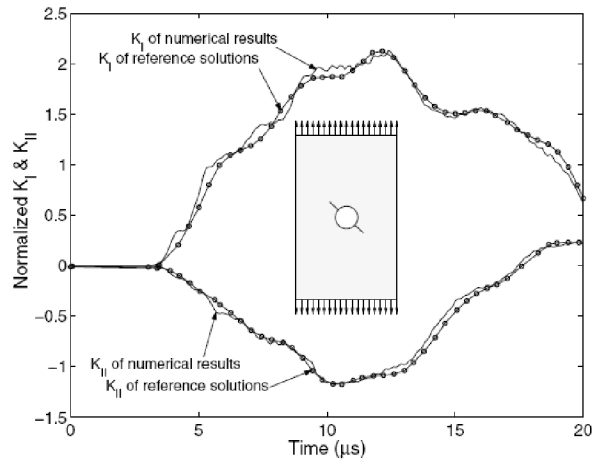


FIGURE 2. The comparison between the present numerical results and the reference solutions [15].

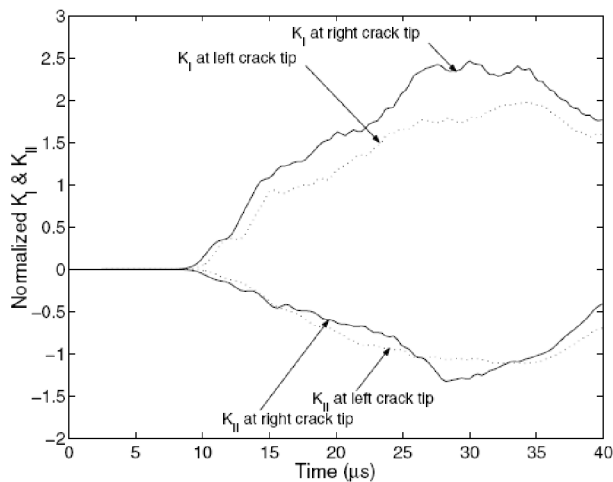


FIGURE 3. Normalized mixed-mode DSIFs at both the left and right crack tips for nonhomogeneous materials.

## CONCLUSIONS

Dynamic fracture behavior for both homogeneous and nonhomogeneous materials is examined in this study. Due to superior features of the M-integral compared to the DCT and the standard J-integral, the current M-integral is extended to incorporate

material nonhomogeneity and dynamic effects. The M-integral consists of actual fields obtained from finite element analysis and auxiliary fields by Williams' solution. The non-equilibrium formulation of the M-integral is employed to evaluate DSIFs. The homogeneous rectangular plate with cracks emanating from a circular hole is employed to verify the numerical implementations. The predicted DSIFs are found to be in good agreement with the reference solutions. Material nonhomogeneity used in the reference is adopted to explore the influence of material nonhomogeneity and dynamic effects on the variation of DSIFs.

## ACKNOWLEDGMENTS

We are grateful to the support from SemMaterials (previously Koch Materials) and the National Science Foundation (NSF) through the GOALI project CMS 0219566 (Program Manager, P.N. Balaguru). Any opinion expressed herein are those of the writers and do not necessarily reflect the views of the sponsors.

## REFERENCES

1. Y. M. Chen, *Engineering Fracture Mechanics*, **7**(4), 653-660 (1975).
2. K. Kishimoto, S. Aoki, and M. Sakata, *Engineering Fracture Mechanics*, **13**(2), 387-394 (1980).
3. V. Murti, and S. Valliappan, *Engineering Fracture Mechanics*, **23**(3), 585-614 (1986).
4. Y. J. Lee and L. B. Freund, *ASME Journal of Applied Mechanics*, **57**(1), 104-111 (1990).
5. J. Dominguez and R. Gallego, *International Journal for Numerical Methods in Engineering*, **33**(3), 635-647 (1992).
6. P. Krysl and T. Belytschko, *International Journal for Numerical Methods in Engineering*, **44**(6), 767-800 (1999).
7. C.-E. Rousseau and H. V. Tippur, *Mechanics of Materials*, **33**(7), 403-421 (2001).
8. M. L. Williams, *ASME Journal of Applied Mechanics*, **24**(1), 109-114 (1957).
9. V. Parameswaran and A. Shukla, *Mechanics of Materials*, **31**(9), 579-596 (1999).
10. ABAQUS, Version 6.2, H.K.S. Inc., Pawtucket, RI, 2002.
11. C.-C. Wu, P. He and Z. Li, *Computers and Structures*, **80**(5/6), 411-416 (2002).
12. J.-H. Kim and G. H. Paulino, *International Journal for Numerical Methods in Engineering*, **58**(10), 1457-1497 (2003).
13. S. H. Song and G. H. Paulino, *International Journal of Solids and Structures*, **43**(16), 4830-4866 (2006).
14. S. H. Song, "Evaluation of dynamic stress intensity factors for homogeneous and nonhomogeneous materials using the interaction integral method", M.S. Thesis, University of Illinois, 2003.
15. P. Fedelinski, M. H. Aliabadi, and D. P. Rooke, *International Journal of Fracture*, **65**(4), 369-381 (1994).